



# HHS Public Access

Author manuscript

*Mol Immunol.* Author manuscript; available in PMC 2016 December 01.

Published in final edited form as:

*Mol Immunol.* 2015 December ; 68(2 0 0): 203–212. doi:10.1016/j.molimm.2015.08.008.

## Studies of the TLR4-associated protein MD-2 using yeast-display and mutational analyses

Daiva M. Mattis<sup>1</sup>, Adam Chervin<sup>1</sup>, Diana Ranoa<sup>2</sup>, Stacy Kelley<sup>2</sup>, Richard Tapping<sup>2</sup>, and David M. Kranz<sup>1</sup>

<sup>1</sup>Department of Biochemistry, University of Illinois, Urbana, IL 61801, USA

<sup>2</sup>Department of Microbiology, University of Illinois, Urbana, IL 61801, USA

### Abstract

Bacterial lipopolysaccharide (LPS) activates the innate immune system by forming a complex with myeloid differentiation factor 2 (MD-2) and Toll-like receptor 4 (TLR4), which is present on antigen presenting cells. MD-2 plays an essential role in this activation of the innate immune system as a member of the ternary complex, TLR4:MD-2:LPS. With the goal of further understanding the molecular details of the interaction of MD-2 with LPS and TLR4, and possibly toward engineering dominant negative regulators of the MD-2 protein, here we subjected MD-2 to a mutational analysis using yeast display. The approach included generation of site-directed alanine mutants, and ligand-driven selections of MD-2 mutant libraries. Our findings showed that: 1) proline mutations in the F119-K132 loop that binds LPS were strongly selected for enhanced yeast surface stability, 2) there was a preference for positive-charged side chains (R/K) at residue 120 for LPS binding, and negative-charged side chains (D/E) for TLR4 binding, 3) aromatic residues were strongly preferred at F119 and F121 for LPS binding, and 4) an MD-2 mutant (T84N/D101A/S118A/S120D/K122P) exhibited increased binding to TLR4 but decreased binding to LPS. These studies revealed the impact of specific residues and regions of MD-2 on the binding of LPS and TLR4, and they provide a framework for further directed evolution of the MD-2 protein.

### Keywords

Lipopolysaccharide; MD-2; Toll-like receptor-4; Yeast display

---

To whom correspondence should be addressed: David M. Kranz, d-kranz@illinois.edu.

#### Conflict of interest

The authors declare no competing financial interests.

The content is solely the responsibility of the authors and does not necessarily represent the official views of the National Institutes of Health.

**Publisher's Disclaimer:** This is a PDF file of an unedited manuscript that has been accepted for publication. As a service to our customers we are providing this early version of the manuscript. The manuscript will undergo copyediting, typesetting, and review of the resulting proof before it is published in its final citable form. Please note that during the production process errors may be discovered which could affect the content, and all legal disclaimers that apply to the journal pertain.

## 1. Introduction

Lipopolysaccharide (LPS), endotoxin, is found on the outer membrane of most gram-negative bacteria. LPS is able to potently stimulate the innate immune system through interaction with Toll-like receptor 4 (TLR4) on the surface of antigen presenting cells (APCs) (Medzhitov et al., 1997). TLR4 activation by LPS induces the release of cytokines such as IL-1, IL-6 and TNF- $\alpha$ . While these cytokines activate the innate immune system to facilitate elimination of infectious agents, higher levels of gram-negative bacteria, especially systemically, can lead to widespread vasodilation, hypoperfusion, and myocardial dysfunction. These can result in an overwhelming hyper-inflammatory response known as systemic inflammatory response syndrome (SIRS), leading to septic shock.

LPS is thought to be delivered to an APC subsequent to bacterial cell lysis and/or by removal from the bacteria surface by LPS-binding protein (LBP). LBP facilitates LPS delivery to CD14, which in turn allows LPS to associate with either myeloid differentiation factor 2 (MD-2) directly, or with the complex of MD-2 and TLR4 on the cell surface. MD-2 is a 160 amino acid glycoprotein that contains an N-terminal secretion signal; it consists of two beta sheets that form a deep hydrophobic cavity (Ohto et al., 2007). Crystal structures of MD-2 with LPS variants have aided in understanding how the two molecules interact. MD-2 is able to accommodate five acyl chains of LPS in its hydrophobic cavity, leaving the phosphorylated glucosamine backbone of LPS extending from this pocket (Park et al., 2009). MD-2 is essential for LPS-mediated activation of TLR4, as MD-2 deficient mice are unable to respond to LPS (Nagai et al., 2002).

LPS consists of the bacterial cell membrane-anchored toxic fatty acid (lipid A) common to all gram-negative bacteria, a core oligosaccharide region, and a complex polysaccharide coat (O antigen) that varies among species. The LPS produced by bacteria vary not only in presence or absence of the O antigen, but may also vary in phosphate patterns, number of acyl chains, and lipid A composition (Akira et al., 2006). Lipid A and the phosphates of LPS are required for binding to MD-2 and TLR4, but LPS is capable of binding to MD-2 without the O antigen (Kohara et al., 2006). Only recently has the core oligosaccharide region been shown to play a role in MD-2 binding (Ittig et al., 2012).

Although the molecular details of TLR4 activation are not completely understood, a crystal structure of the TLR4:MD-2:LPS complex has guided the present model (Park et al., 2009). In one scenario, the MD-2:LPS complex binds to cell surface TLR4, which is thought to dimerize with a second TLR4, thus forming a dimer of trimers (TLR4:MD-2:LPS)<sub>2</sub>. As observed in other TLR structures, the two TLR4 molecules interact at the C-termini with the N-termini directed away from each other. The ternary crystal structure shows direct contacts between TLR4 and MD-2 and between TLR4 and LPS (Park et al., 2009). Dimerization is thought to be required for signaling through the TIR domain, leading to activation of transcription factors such as nuclear factor  $\kappa$ B (NF- $\kappa$ B), and the release of inflammatory molecules such as IL-1 and TNF $\alpha$ .

The potency of LPS in this process makes it capable of incapacitation and lethality, and appears responsible for the involvement of LPS in multiple illnesses. While perhaps best

known as a cause of endotoxic shock, in recent years, TLR4 activation by LPS has also been proposed to exacerbate other inflammatory conditions such as asthma (Michel et al., 1989). The detailed mechanisms in the latter process remains to be determined, but downstream effects likely involve activation of T<sub>H2</sub> cells and subsequent production of IgE and allergy related inflammatory cytokines (Herrick and Bottomly, 2003). Low levels of LPS have been shown to induce T<sub>H2</sub> cells, while high levels of LPS induce T<sub>H1</sub> activation (Eisenbarth et al., 2002). The allergen Derp2 from the dust mite has been shown to be structurally homologous to MD-2 and to bind to LPS, suggesting that it may act as a ligand in both the innate and adaptive systems (Trompette et al., 2009; Wills-Karp et al., 2010).

In studies to date, MD-2 has been examined by selective mutagenesis using predominantly single-site alanine mutations at several residues, followed by expression and purification of the soluble mutants. It is a challenge to generate monomeric soluble MD-2 protein, and mammalian and insect cell systems have been used to accomplish protein expression (Teghanemt et al., 2008b). In order to develop a more rapid, higher throughput system for analysis of MD-2, we used yeast display of the human MD-2 as a fusion protein. Accordingly, we displayed human MD-2 on the surface of yeast, and showed that the displayed protein could bind to MD-2-specific monoclonal antibodies (mAbs) and to its ligands, LPS and human TLR4. Guided by the structure of MD-2 in complex with LPS and TLR4, we generated various alanine mutants to examine the role of specific residues in ligand binding. We also generated and screened several libraries of mutants (with up to 10<sup>7</sup> independent transformants) that allowed us to identify key residues and to isolate MD-2 mutants improved in either stability (i.e. surface levels) or ligand binding.

## 2. Materials and Methods

### 2.1 Yeast display cloning and libraries

The gene for MD-2 was synthesized by Genscript and sub-cloned into the yeast display vector pCT302, which contains an N-terminal Hemagglutinin (HA) tag and a C-terminal Myc (c-myc) tag, using restriction sites *NheI* and *XhoI* (Boder and Wittrup, 2000). Mutants of MD-2 were engineered by site directed mutagenesis using QuickChange as described by the manufacturer (Stratagene, La Jolla, CA). The following mutants were constructed: L54A, F119A, F121A, I124A, F126A, F131A, D100A, D101A, and E92V/S118P. The E92V and S118P mutations were cloned individually into MD-2. After verifying mutations by sequencing, plasmids were transformed into EBY100 cells.

Three libraries of mutants were made in the human pCT302:D101A mutant. One library consisted of error-prone PCR-based mutations and two libraries consisted of site-directed mutants constructed in the LPS binding region of MD-2. The latter two libraries were constructed by site-directed mutagenesis using overlapping degenerate primers (with NNS codons) in the following groups of four residues of MD-2: (118–121) and (118/120/122/123). The error prone library was generated by amplifying the gene MD-2:D101A from the pCT302:D101A plasmid using flanking primers with a method of error-prone PCR to give a 0.5% error rate (Richman et al., 2009). The PCR products were transformed along with the *NheI*/*BglII* digested plasmid pCT302 into the yeast strain EBY100 (Boder and Wittrup, 2000), which inserts the PCR product into the plasmid by

homologous recombination (Starwalt et al., 2003; Jones et al., 2006). The libraries were cultured in selective media (SD-CAA) for 48 hours. Ten clones from each library were sequenced to ensure the presence of the expected diversity.

## 2.2 Analysis of yeast surface displayed MD-2 with antibodies 4H1 and 18H10

Expression of Aga2p fusions on yeast was induced by growth in medium containing galactose at 20°C for 32–48 hours. After induction, yeast were stained with anti-c-myc mAb 9E10 at 1:100 dilution (Invitrogen) or anti-HA mAb HA.11 at 1:50 dilution (Covance). The anti-HA stained cells were stained with secondary goat-anti-mouse antibody at 1:200 dilution (Invitrogen) and the anti-c-myc stained cells were stained with secondary goat-anti-chicken at 1:100 dilution (Invitrogen). C-myc and HA tag expression were used to estimate surface expression of clones. After induction, the surface displayed MD-2 was also analyzed using two monoclonal anti-MD2 antibodies (mAbs). Yeast cells ( $1 \times 10^6$ ) were incubated with mAb 4H1 at 1:200 dilution (Hycult biotech) or mAb 18H10 at 1:100 dilution (Hycult biotech) for one hour on ice. Cells were washed with 200ul Phosphate Buffer Saline + 0.5% Bovine Serum Albumin (PBS+0.5%BSA) followed by goat anti-mouse Alexafluor 647 (GaM647) at 1:200 dilution (Invitrogen) on ice for one hour. Cells were washed and analyzed on an Accuri C6 flow cytometer.

## 2.3 Human CD14 and TLR4 protein construction, expression, and purification

Human soluble CD14 (amino acids 1-337) was cloned and expressed as previously described (Kelley et al., 2013), and purified as previously described (Ranoa et al., 2013). Briefly, human soluble CD14 was amplified from genomic DNA and cloned into a pDisplay vector containing a thrombin cleavage site (LVPRGS) and the Fc domain of human IgG1. Site-directed mutagenesis (C306S) via primer extension was conducted to avoid unnatural disulfide bonding resulting from the truncated coding region of our construct. The final construct was sequenced (University of Illinois Urbana-Champaign Sequencing Center). Human soluble CD14 protein was purified from stable HEK 293F cell (Invitrogen) supernatant following transfection via protein G affinity chromatography, thrombin cleavage, protein A affinity chromatography, and size exclusion chromatography. Following size exclusion, fractions containing human soluble CD14 were pooled, concentrated using an Amicon Ultra-4 unit (Millipore), and stored at 4 °C. The resulting human soluble CD14 (amino acids 1-337; C306S) protein is bioactive as measured by LPS binding activity and the ability to facilitate LPS-induced IL-8 production from human epithelial SW620 cells (Kelley et al., 2013).

Soluble human TLR4 extracellular domain (ECD) was generated by following the hybrid LRR technique first described by Kim *et al.* 2007 and adopted by Guan *et al.* 2010 (Kim et al., 2007; Guan et al., 2010). Briefly, the gene for TLR4 ECD region (aa 27-527) was fused to the LRR C-terminal capping module (aa 133-200) of the hagfish variable lymphocyte receptor (VLRB.61 clone). The gene product was cloned as a BglII/NheI fragment into a modified pDisplay vector containing a Flag-tag upstream of the BglII site and an Fc domain of the human IgG1 downstream of the NheI site. A thrombin cleavage site (LVPRGS) was inserted between the 3' end of the TLR4 hybrid gene and the 5' end of the Fc region to allow cleavage of the soluble TLR4 from the Fc fusion protein. Stable HEK 293F cell lines

expressing recombinant soluble TLR4-ECD-Fc fusion proteins were generated by G418 selection and limiting dilution as previously described (Guan et al., 2010). Stable cell lines were maintained in Freestyle serum-free expression medium (Invitrogen) supplemented with 0.25mg/ml G418 and cultured in suspension at 37°C with continuous shaking at 125 rpm in a humidified environment containing 8% CO<sub>2</sub>.

Soluble TLR4-ECD-Fc was purified from stable HEK 293F cell supernatant by affinity chromatography using Protein G sepharose for fast flow on an AKTA prime purification system (GE Healthcare), as previously described (Guan et al., 2010). The Fc tag was removed after the first round of purification by adding a restriction grade thrombin protease (Novagen) at a concentration of 1U thrombin per 0.25mg TLR4-ECD-Fc protein. After 18 hours incubation at room temperature, the TLR4-ECD was separated from the Fc fragments by another round of affinity chromatography in the AKTA prime system using a 1ml pre-packed protein A column (Pierce) and PBS pH 7.4 running buffer. The TLRs were concentrated from the flow-through using an Amicon Ultra-4 centrifugal device (Millipore) and centrifuged at 2500×g for 15–25 minutes at 4°C, until the volume was reduced to 0.5ml. The concentrated protein was then injected into a Superdex 200 10/300GL gel filtration column (GE Healthcare) in PBS pH 7.4 running buffer at a flow rate of 0.5 ml/min. The eluted fractions containing monomeric TLR4 ECD were pooled and concentrated using the Amicon Ultra-4 centrifugal device. Final protein concentration after three rounds of purification was measured using the Pierce BCA protein assay kit. The protein yield for recombinant soluble TLR4 ECD was 0.3mg per liter of media.

The purified TLR4 ECD was properly folded as evidenced by its ability to bind to a microtiter plate coated with a conformational-dependent anti-TLR4 monoclonal antibody (clone HTA 125; eBioscience). Binding of TLR4 ECD to the mAb was detected using HRP-conjugated anti-Flag antibody (clone M2; purchased from Sigma) followed by the addition of o-phenylenediamine (OPD) substrate (Pierce). Purified soluble TLR4 did not exhibit any cross reaction with other anti TLR mAbs (anti-TLR1 clone GD2F4, anti-TLR2 clone T2.5, anti-TLR6 clone hPer6, and anti-TLR10 clone 3C10C5).

#### 2.4 Binding of yeast displayed MD-2 and mutants to biotin-LPS and TLR4

Yeast cells with the Aga2p fusion were induced. After 10 minutes of vigorous vortexing, 100nM biotin-LPS (biotinylated ultra-pure LPS-EB, InvivoGen; LPS concentration was based on a formula weight of biotin-LPS of approximately 10,000) was incubated at a 1:3 molar ratio with human CD14 in a 37°C water bath for one hour. Biotin-LPS/CD14 was then added at various concentrations to  $1 \times 10^6$  yeast cells and incubated at 37°C for one hour. Cells were washed and incubated with SA-Alexafluor647 (SA647). After washing, cells were analyzed on an Accuri C6 flow cytometer.

To detect TLR4 binding,  $1 \times 10^6$  yeast cells were incubated with various concentrations of flag-tagged TLR4, and after washing with PBS+0.5%BSA, the cells were incubated with anti-human TLR4 mAb HTA-125 at a 1:200 dilution (eBioscience). After one hour on ice, cells were washed and incubated with GaM647. After washing, cells were analyzed on an Accuri C6 flow cytometer. A negative control included yeast displayed protein L3, which is a V $\beta$  domain with approximately the same size as MD-2 (Mattis et al., 2013).

## 2.5 Selection of MD-2 mutant libraries by fluorescence-activated cell sorting (FACS)

Aga2p fusions were induced by growth of yeast cells in medium containing galactose at 20°C for 32–48 hours. After induction, yeast-displayed MD-2 proteins were selected by FACS on a BD FACS Aria II high-speed cell sorter or analyzed by flow cytometry. Yeast cell libraries (approximately  $1 \times 10^8$  cells) were selected using an equilibrium based methodology. The LPS libraries were incubated with the described concentration of biotin-LPS/CD14 at 37°C, washed, and then incubated with SA647. Following each sort, the cells were grown in selective SD-CAA media, and then induced. Each of the LPS sorts collected the top 1% of cells. The 1<sup>st</sup> sort selected with 5ug/ml biotin-LPS/CD14, the 2<sup>nd</sup> sort with 1ug/ml biotin-LPS/CD14, and the 3<sup>rd</sup> through 5<sup>th</sup> sorts with 0.1 ug/ml biotin-LPS/CD14. Cells from the 5<sup>th</sup> sorts were plated and grown on selective media and 10 clones from each of the 5<sup>th</sup> sorts sequenced.

The four-codon library of residues (118/120/122/123) was sorted a second time selecting clones for binding to TLR4. The cells were incubated with the following described concentration of TLR4 on ice, washed, incubated with HTA-125, washed, incubated with GaM647, washed, and selected by FACS. For the 1<sup>st</sup> sort, the cells were stained with 10ug/ml TLR4 and the top 1% of cells collected, 10ug/ml TLR4 for the 2<sup>nd</sup> sort and the top 0.5% of cells collected, 5ug/ml TLR4 for the 3<sup>rd</sup> sort and the top 0.1% of cells collected, 1ug/ml of TLR4 for the 4<sup>th</sup> sort and the top 0.2% of cells collected, and 1ug/ml TLR4 for the 5<sup>th</sup> and final sort and the top 0.4% of cells collected. Cells from the 4<sup>th</sup> and 5<sup>th</sup> sorts were plated and grown on selective media and sequenced. Clones from all of the libraries were analyzed for equilibrium binding to biotin-LPS/CD14 and TLR4. C-myc and HA tag expression were used to estimate surface expression of clones. Cells were analyzed on a BD Accuri C6 flow cytometer.

## 3. Results

### 3.1 Yeast display expression and detection of MD-2

To determine whether the yeast display system could be used to examine various features of the MD-2 protein, the human MD-2 gene was cloned as an Aga-2 fusion into yeast display vector pCT302 (Fig. 1A) (Boder and Wittrup, 2000). Expression of the full-length Aga-2/MD-2 fusion on the surface of yeast, as well as a control fusion called L3 that contains a T cell receptor V $\beta$  domain of similar size to MD-2, (Mattis et al., 2013) was confirmed by screening with antibodies for the HA tag at the N-terminus and c-myc tag at the C-terminus of the protein (Fig. 1B). To detect the MD-2 protein itself, yeast cells were stained with two monoclonal antibodies (mAbs) to human MD-2, 4H1 and 18H10. Both mAbs 4H1 and 18H10 bound to the MD-2 fusion on the yeast surface, but not to the L3 fusion (Fig. 1C). These results confirm that MD-2 is expressed on the surface and they suggest that a substantial fraction of it is folded properly.

### 3.2 Binding of yeast displayed MD-2 to LPS

To examine if LPS binding to yeast-displayed MD-2 could be detected, yeast cells were incubated with biotin-LPS. Since CD14 has been shown to facilitate binding of LPS to MD-2, we conducted experiments with both the preincubated biotin-LPS/CD14 complex



and biotin-LPS alone (Figs. 2A & B). The biotin-LPS demonstrated a positive peak (solid line open histogram) in comparison to secondary reagent only (grey filled histogram)(Fig. 2A). The biotin-LPS also showed a minor degree of nonspecific binding to the negative control yeast (L3) as seen as a shoulder (dotted line) (Fig. 2A). However, this weakly positive shoulder (L3) was eliminated in the presence of the preincubated biotin-LPS/CD14 complex (Fig. 2B), while the complex mixture retained binding to yeast-displayed MD-2 (Fig. 2B). This result is consistent with the possibility that aggregated LPS, more abundant in the absence of CD14, yielded some background association with the yeast. To avoid this and deliver LPS more naturally, subsequent experiments were performed using biotin-LPS preincubated with CD14.

In order to estimate the approximate affinity of the measured interaction between MD-2 and LPS, various concentrations of biotin-LPS/CD14 were incubated with MD-2 and then examined by flow cytometry. The mean fluorescence units (MFU) for histograms were determined at each concentration of LPS, and the background MFU was subtracted from these values. In order to estimate the equilibrium binding affinity, the concentration of LPS was determined by assuming an average molecular weight of 10,000gm/mol. Using this approach, the yeast-displayed MD-2 was estimated to bind to the biotin-LPS/CD14 with a  $K_D$  value of 90 nM (Fig. 2C). This estimate of affinity is similar to the  $K_D$  value of 65 nM described by Kirkland and colleagues for a soluble form of MD-2 (Viriyakosol et al., 2001). Other studies have found picomolar binding affinities of the TLR4/MD-2/endotoxin complex, when endotoxin was first incubated with LBP and CD14, creating apparent monomeric endotoxin/CD14 complexes (Gioannini et al., 2004; Prohinar et al., 2007; Gioannini et al., 2014). This indicates that the LPS in our experiments may be partially aggregated, as suggested above.

### 3.3 Binding of yeast displayed MD-2 to TLR4

To examine if yeast-displayed MD-2 binding to TLR4 could be detected, a TLR4-extracellular domain-Fc fusion protein was expressed, purified, and the Fc tag removed, followed by another round of purification to yield soluble monomeric TLR4-extracellular domain (TLR4). Although TLR4 was purified as a monomer, it is possible that the monomer preparations may retain divalent forms and consequently the affinity calculations are estimates. After titration with various concentrations of TLR4, the TLR4-specific antibody HTA-125 was used to detect TLR4 binding. The TLR4 demonstrated a positive peak (solid line open histogram) in comparison to the negative control yeast L3 (dotted line) and the secondary reagent only (grey filled histogram) (Fig. 3A).

To estimate the approximate affinity of MD-2 and TLR4, various concentrations of TLR4 were incubated with MD-2 and then examined by flow cytometry. The MFU for histograms was determined as described in subsection 3.2 for LPS. The concentration of TLR4 was determined by assuming an average molecular weight of 80,000gm/mol. Using this method, the yeast-displayed MD-2 was estimated to bind to TLR4 with a  $K_D$  value of 100nM (Fig. 3B). This estimate of affinity is within an order of magnitude of the affinity measured by Golenbock and colleagues for soluble MD-2, with an apparent  $K_D$  for TLR4 of 12nM (Visintin et al., 2005).

### 3.4 Ligand binding analysis of yeast-displayed alanine mutants of MD-2

Several studies have suggested that MD-2 residues in the region F119 to K132 are important for LPS binding to MD-2 (Re and Strominger, 2003; Kobayashi et al., 2006; Teghanemt et al., 2008a). In addition, this region has been shown to be in contact with an LPS ligand present in the crystal structure of the MD-2 complex ((Park et al., 2009), Fig. 4A). To examine if the MD-2/yeast display system could be used as a platform to more rapidly examine the role of MD-2 residues in ligand binding, various MD-2 residues were mutated to alanine: L54A, F119A, F121A, I124A, F126A, and Y131A (Tsuneyoshi et al., 2005; Kobayashi et al., 2006; Park et al., 2009). Each of the mutants was titrated with various concentrations of the biotin-LPS/CD14 complex (Fig. 5A). Such titrations can yield two flow cytometry parameters that provide information about the mutant. First, the maximum MFU at the highest ligand concentrations can be an indicator of the stability of the protein (i.e. higher yeast surface levels are correlated with greater stability of the protein or mutant) (Kieke et al., 1999; Shusta et al., 1999). Second, the concentration of ligand that yields 50% maximal binding is correlated with the equilibrium binding affinity (Kieke et al., 2001; Feldhaus et al., 2003).

Based on the titrations with LPS, mutants F126A and Y131A showed no difference in stability (maximum level of surface display, MFU) or affinity, relative to MD-2. In contrast, the two mutants F121A and F119A showed the most significant impact on both surface levels and apparent affinity for LPS. Mutants I124A and L54A showed an intermediate impact on LPS binding, in terms of both stability and apparent affinity. Consistent with these results, mutants F119A and F121A (Tsuneyoshi et al., 2005), and the double mutant F121A/K122A (Teghanemt et al., 2008a), have been reported to reduce LPS binding activity mediated by MD-2. This previous study showed that double mutant Y131A/K132A was unable to bind to LPS, although the single-site mutant K132A (the single-site Y131A mutant was not tested) was able to partially bind LPS (Teghanemt et al., 2008a). Mutant F126A was previously shown to still bind its ligands, but not activate TLR4 (Teghanemt et al., 2008a). Although residues L54, I124, F126, and Y131 were proposed to contribute hydrophobic bonds with LPS acyl chains (Park et al., 2009), the results here may indicate these interactions with LPS play less of a role in stability and affinity of MD-2 in comparison to F121 and F119. Both F119 and F121 are located at the opening of the MD-2 pocket that LPS inserts into, and therefore these residues appear to have more potential to impact the interaction with LPS; in contrast, Y131, F126, I124, and L54 are located deeper inside of the MD-2 pocket, limiting their potential interactions to a smaller region of LPS. In the case of F126 and Y131, this interaction is limited to the tails of the LPS lipid chains.

Another region of the MD-2 molecule, involving residues D100 and D101, has been proposed to impact TLR4 binding, but not association with LPS (Re and Strominger, 2003). To determine if we could verify and extend these observations by analysis of yeast-displayed MD-2, the single-site mutants D100A and D101A were generated. As expected, these two mutants showed statistically significant reduced binding to TLR4 (Fig. 5B), but their binding to LPS remained the same as the wild type MD-2 (Fig. 5C). The observation that maximum surface levels were shown to be the same with LPS provided further evidence



that these two mutants were expressed properly and thus the reduction in TLR4 binding was indeed due to a loss of important contacts.

### 3.5 Use of yeast display libraries for analysis and engineering of LPS binding

To further understand the role that particular residues play in MD-2 function, we went beyond single-site alanine mutations and engineered libraries of mutants that would contain every amino acid at several positions. The libraries were then sorted with LPS to isolate mutants that retained, or had improved, binding to the ligand. Two libraries that were degenerate at four codons encoding amino acids adjacent to the key residues identified from the alanine mutants were generated (Fig. 4A). One library contained degenerate codons in positions S118/S120/K122/G123 (called LPS-I library) and the other library contained degenerate codons in positions S118/F119/S120/F121 (called LPS-II library). In addition, a random mutagenic library (LPS-EP) generated by error-prone PCR (with a 0.5% error rate) was also generated in order to determine if any improved LPS-binding mutants could be isolated without regard to the specific residues identified by site-specific analysis. Since this approach focused on the interaction of MD-2 with LPS, the D101A mutant, which showed wild-type binding affinity with no statistically significant difference from MD-2 for LPS binding (Fig. 5C), it was used as the template.

The four-codon libraries and the error prone library were each subjected to FACS through five successive sorts and the top 1% of cells binding to biotin-LPS/CD14 was selected. The selecting concentrations were: 5ug/ml biotin-LPS/CD14 for the 1<sup>st</sup> sort, 1ug/ml for the 2<sup>nd</sup> sort, and 0.1 ug/ml for the 3<sup>rd</sup> through 5<sup>th</sup> sorts. After the final sort, cells were plated and ten colonies from each library were analyzed for binding to biotin-LPS/CD14 and sequenced. Three unique mutants from the LPS-I library, two unique mutants from the LPS-II library, and three unique mutants from the LPS-EP library were identified among these clones (Fig. 6).

Stringent selection of yeast display libraries with ligands is an approach to identify those residues within a library that represent key contacts or that can compensate for other mutations (Wang et al., 2010). To examine if any mutants from our libraries could compensate for the decreased binding of mutation MD-2/D101A to TLR4, the LPS-I library (118/120/122/123) was subjected to FACS through five successive sorts with the following concentrations of TLR4: 10ug/ml TLR4 for the 1<sup>st</sup> and 2<sup>nd</sup> sorts, 5ug/ml TLR4 for the 3<sup>rd</sup> sort, and 1ug/ml TLR4 for the 4<sup>th</sup> and 5<sup>th</sup> sorts. The 4<sup>th</sup> and 5<sup>th</sup> sorts were plated and eight clones from the 4<sup>th</sup> sort and 10 clones from the 5<sup>th</sup> sort were sequenced. The 4<sup>th</sup> sort contained six unique mutants, and the 5<sup>th</sup> sort a single unique mutant (TLR4-selected), that was also identified in the 4<sup>th</sup> sort (Fig. 6).

### 3.6 Binding of library-derived mutants to LPS and TLR4

Representatives of each of the mutants from the biotin-LPS/CD14 and TLR4 selected libraries were examined for binding to both LPS and TLR4. To verify that these mutants could bind biotin-LPS/CD14 and TLR4, they were titrated with various concentrations of the biotin-LPS/CD14 complex and TLR4 (Fig. 7). As discussed above in subsection 3.4, these titrations provide two parameters of interest, the maximum MFU at the highest ligand

concentrations as an indicator of the stability of the protein (Kieke et al., 1999; Shusta et al., 1999) and the concentration of ligand that yields 50% maximal binding as an indicator of the equilibrium binding affinity (Kieke et al., 2001; Feldhaus et al., 2003).

In comparison to MD-2, the mutants did not differ significantly in their binding affinities for biotin-LPS/CD14, with the exception of the TLR4-selected mutant (T84N/D101A/S118A/S120D/K122P) (Fig. 7). This mutant did not reach saturation levels of binding to biotin-LPS/CD14, suggesting that it may have a reduced binding affinity relative to MD-2. However, the maximum MFU and hence stability of all the mutants was improved over MD-2 regardless of the ligand used for selection. The relative improvements in stability, confirmed using both the LPS/CD14 and TLR4 ligands, appeared to correspond to the origin of the library that yielded the mutants: LPS-EP mutants had the most improved stability, followed by LPS-II, and then LPS-I (Figs. 7A and 7B).

The TLR4-selected mutant showed the most significant increase in yeast surface display, with a 3-fold higher MFU than the next highest group of mutants, from the LPS-EP library (Fig. 7B). The large improvement in maximum MFU with minimal changes in binding affinity suggested that improvements in protein stability are likely responsible for the selection of these mutants. Nevertheless, the retention in binding to each of the ligands verifies that these mutants have selected residues that maintain, or possibly improve, the requisite contacts.

### 3.7 Sequences of library-derived mutants

The sequences of selected mutants revealed the amino acid positions within the libraries had either maintained the wild-type residues or evolved toward highly restricted side chains. From the ten sequenced mutants of library LPS-I there were three unique sequences (Fig. 6). Six of the ten contained the mutations S118P/S120R/K122P/G123R, two of the ten contained the same mutations except the glycine at position 123 was mutated to an arginine (G123R), and two of the ten contained an S120K mutation rather than the S120R mutation (S118P/S120K/K122P/G123R).

The LPS-II library yielded one clone of ten that contained the mutations S118P/F119Y/S120V, along with the wild-type residue F121. The other nine clones contained the mutations S33Y/S118P/F121W along with the wild-type residues F119 and S120 (Fig. 6). The error-prone library LPS-EP yielded three unique clones, all containing the mutations S118P and E92V. Seven of the ten sequenced clones contained only these two mutations (Fig. 6). Two clones also contained mutation H155R and one clone also contained mutations V113I and L146F.

Although the selected clones retained some wild-type residues in the degenerate library positions, there were clearly strong preferences for certain mutations at other positions. For example, all of the LPS-selected clones, and four of the TLR4-selected clones, contained the S118P mutation. Other LPS-selected mutations that predominated among clones included the LPS-EP mutation E92V and the LPS-I mutation K122P. In addition, all of the clones in the LPS-I library preferentially selected a positive-charged residue at position 120 (S120R or S120K) and position 123 (G123K or G123R). The LPS-II library had less improvement in

stability than either the LPS-EP or LPS-I libraries, and showed preference for either wild-type residues at positions F119 and F121, or a large hydrophobic residue (Fig. 6). These are the same residues that when mutated to alanine had decreased stability and affinity to biotin-LPS/CD14 (Fig. 5A), suggesting that the wild-type phenylalanine or a similarly large hydrophobic residue, such as tyrosine or tryptophan, is preferred at these locations.

In comparison to LPS-selected mutants, the TLR4-selected mutant showed both similarities and a distinct pattern of residue selection. All of the TLR4-selected clones contained the mutation K122P, which was also present in all clones from the same library (LPS-I) selected with biotin-LPS/CD14. Although the S118P mutation present in all LPS-selected mutants was not selected in the 5<sup>th</sup> and final sort of the TLR4-selected mutant, it was present in four of the six unique mutants from the 4<sup>th</sup> sort. Most strikingly, there was a strong preference for negative-charged residues in positions S120 and G123 in the TLR4-selected clones. This preference is in contrast to the LPS-selected mutants that contained positive-charged residues at these two positions.

### 3.8 Role of selected mutations in yeast display surface levels and ligand binding

To examine the influence of several selected mutations on surface display and binding, we generated the individual mutants S118P and E92V, and the double mutant, in the wild-type MD-2, without the D101A mutation. Both S118P and E92V/S118P had statistically significant increased maximum MFU in biotin-LPS/CD14 and TLR4 binding (Fig. 8). Mutant E92V did not reach saturation in either biotin-LPS/CD14 or TLR4 binding at the concentrations used. The maximum MFU for the double mutant E92V/S118P as determined with biotin-LPS/CD14 and TLR4, was improved compared to either mutation individually, indicating these acted synergistically. The improved binding affinity for biotin-LPS/CD14 was statistically significant only for mutant E92V/S118P (Fig. 8A). The predominant effect of these mutations on binding with TLR4 and biotin-LPS/CD14 was on surface stability, with some improvement in affinity for biotin-LPS/CD14 when both mutations are present.

## 4. Discussion

In the present study, we used a system that allows more rapid analysis of the role of specific MD-2 residues in ligand binding than previous studies. In order to develop a more rapid, higher throughput system for analysis of MD-2, we used yeast display of the human MD-2 as a fusion protein. This system allowed us to survey the contribution of residues in single positions, or a group of residues, to ligand binding. We engineered MD-2 mutants from degenerate libraries by random mutagenesis throughout the protein and in selected regions of MD-2 predicted to be involved in ligand binding, targeting primarily the 119–132 loop (Re and Strominger, 2003; Kobayashi et al., 2006; Teghanemt et al., 2008a). The results provided insight into the role of specific residues in MD-2 stability and ligand binding, and they showed that yeast-displayed MD-2 could serve as a system for further engineering.

Proline mutations at positions S118 and K122 suggested that these conferred stability to the protein, or to that region of the protein. The strong preference for these prolines was also indicated by the observation that different degenerate codons for proline were present among the clones isolated from the various libraries. The S118 residue is present at the start

of a loop in MD-2 that connects two beta sheets and is located at the opening of the MD-2 pocket where the LPS acyl chains enter (Fig. 4A). The position is adjacent to the loop region (F119-K132) identified by previous studies as important for interactions with LPS (Re and Strominger, 2003; Kobayashi et al., 2006; Teghanem et al., 2008a). The wild-type serine at this position forms a hydrogen bond with one of the phosphate groups of LPS based on the crystal structure (Park et al., 2009). Although proline at this position eliminates this potential interaction, it likely decreases the conformational entropy within this region and this could lead to an increase in the stability of the protein (Prajapati et al., 2007). The proline substitutions at positions S118 and K122 (Fig. 4) could increase the rigidity in and around the LPS-binding loop (F119-K132), and may position the other selected residues such as S120R and G123R to engage the ligands more effectively.

In addition to the proline mutations S118P and K122P in the LPS-selected library (S118/S120/K122/G123), all mutants contained positive-charged residues at the nearby residues, S120R/K and G123K/R. We propose that positive charges at positions 120 and 123 promote a charge interaction with the negative-charged LPS phosphate groups (Fig. 4B). The lysine at position 122 of the wild-type MD-2 may serve a similar role as discussed in previous studies (Meng et al., 2010a), but the proline mutation at this position could provide a strong requirement that either lysine or arginine be present at the adjacent position 123 in order to compensate. Residue 122 has also been identified by studies as important in endotoxin and MD-2 species specificity interactions (Meng et al., 2010a; Meng et al., 2010b; Ohto et al., 2012; Oblak and Jerala, 2014; Oblak and Jerala, 2015). It is also worth noting that the lysine or arginine at position 123 could potentially form a hydrogen bond with the Ser415 of the second TLR4 molecule (Fig. 4B).

It was striking that while a positive charged residue was predominant at position 120 with LPS-selection, a negative charged residue was predominant at position 120 (S120D) when the library was selected with TLR4 (Fig. 6). Furthermore, position 123 in the TLR4-selected clones either retained the wild-type glycine, or they also contained a negative-charged residue (as opposed to the positive charge observed with LPS-selection). Lee et al have shown that the backbone of G123 forms a hydrogen bond with TLR4 (Park et al., 2009), consistent with the retention of glycine in most of the mutants. However, it is difficult to predict how the negative charged mutations operate to improve the binding to TLR4. The distinct LPS-binding curve of this mutant (TLR4<sup>selected</sup> in Fig. 7A) may indicate that the negative charged side chains reduce the binding to LPS, as might be predicted due to repulsion of the phosphate groups in LPS.

It is also of interest that residues F119 and F121 were highly restricted to wild-type or conserved (Tyr or Trp) residues, indicating a strong preference for aromatic residues. We suggest that the hydrophobic, space-filling property of these side chains facilitates the creating of a pocket for insertion of the hydrophobic LPS acyl chains. Two other mutations, S118P and E92V, identified using an error prone library, appear to operate primarily by stabilizing the protein on the surface of yeast. Such single-site mutations have been observed using random mutagenesis approaches in other proteins engineered by yeast display. While the mechanistic basis of their stabilizing effects are often not clear, the mutations can be of use in expressing the protein at higher levels in secretion systems (Shusta et al., 1999).

## 5. Conclusion

In summary, we show that it is possible to express MD-2 on the surface of yeast, allowing the more rapid analysis of single-site mutants. Through both alanine single-site mutagenesis and library approaches, the system allowed us to determine the critical role of aromatic residues at position 119 (F119) and position 121 (F121) for LPS binding. In addition the selection of prolines at several positions (118 and 122) stabilized the protein, and opposite charged mutations at positions 120 and 123 provided a 'toggle' that yielded improved binding to LPS or TLR4. Finally, there is the possibility that mutants with increased affinity for LPS and decreased affinity for TLR4 (or vice versa) could be potentially used as 'dominant negative' inhibitors of the LPS reactions. Accordingly, directed evolution of MD-2 using yeast display may be of further use in developing such MD-2 reagents, which may be of therapeutic value in the treatment of sepsis.

## Acknowledgments

We thank the staff of University of Illinois Biotechnology Center for assistance in flow sorting and DNA sequencing. This work was supported by National Institutes of Health grants [R21-AI094037 to D.M.K.], and by the National Heart, Lung, and Blood Institute of the National Institutes of Health under Award Number F30-HL096352 [to D.M.M].

## References

- Akira S, Uematsu S, Takeuchi O. Pathogen recognition and innate immunity. *Cell*. 2006; 124:783–801. [PubMed: 16497588]
- Boder ET, Wittrup KD. Yeast surface display for directed evolution of protein expression, affinity, and stability. *Methods Enzymol*. 2000; 328:430–44. [PubMed: 11075358]
- Eisenbarth SC, Piggott DA, Huleatt JW, Visintin I, Herrick CA, Bottomly K. Lipopolysaccharide-enhanced, toll-like receptor 4-dependent T helper cell type 2 responses to inhaled antigen. *J Exp Med*. 2002; 196:1645–51. [PubMed: 12486107]
- Feldhaus MJ, Siegel RW, Opresko LK, Coleman JR, Feldhaus JM, Yeung YA, Cochran JR, Heintelman P, Colby D, Swers J, Graff C, Wiley HS, Wittrup KD. Flow-cytometric isolation of human antibodies from a nonimmune *Saccharomyces cerevisiae* surface display library. *Nature biotechnology*. 2003; 21:163–70.
- Gioannini TL, Teghanemt A, Zhang D, Coussens NP, Dockstader W, Ramaswamy S, Weiss JP. Isolation of an endotoxin-MD-2 complex that produces Toll-like receptor 4-dependent cell activation at picomolar concentrations. *Proc Natl Acad Sci U S A*. 2004; 101:4186–91. [PubMed: 15010525]
- Gioannini TL, Teghanemt A, Zhang D, Esparza G, Yu L, Weiss J. Purified monomeric ligand-MD-2 complexes reveal molecular and structural requirements for activation and antagonism of TLR4 by Gram-negative bacterial endotoxins. *Immunologic research*. 2014; 59:3–11. [PubMed: 24895101]
- Guan Y, Ranoa DR, Jiang S, Mutha SK, Li X, Baudry J, Tapping RI. Human TLRs 10 and 1 share common mechanisms of innate immune sensing but not signaling. *Journal of immunology* (Baltimore, Md : 1950). 2010; 184:5094–103.
- Herrick CA, Bottomly K. To respond or not to respond: T cells in allergic asthma. *Nature reviews Immunology*. 2003; 3:405–12.
- Ittig S, Lindner B, Stenta M, Manfredi P, Zdorovenko E, Knirel YA, dal Peraro M, Cornelis GR, Zahringer U. The lipopolysaccharide from *Capnocytophaga canimorsus* reveals an unexpected role of the core-oligosaccharide in MD-2 binding. *PLoS pathogens*. 2012; 8:e1002667. [PubMed: 22570611]
- Jones LL, Brophy SE, Bankovich AJ, Colf LA, Hanick NA, Garcia KC, Kranz DM. Engineering and characterization of a stabilized alpha1/alpha2 module of the class I major histocompatibility

- complex product Ld. *The Journal of biological chemistry*. 2006; 281:25734–44. [PubMed: 16815841]
- Kelley SL, Lukk T, Nair SK, Tapping RI. The Crystal Structure of Human Soluble CD14 Reveals a Bent Solenoid with a Hydrophobic Amino-Terminal Pocket. *Journal of immunology (Baltimore, Md : 1950)*. 2013; 190:1304–11.
- Kieke MC, Shusta EV, Boder ET, Teyton L, Wittrup KD, Kranz DM. Selection of functional T cell receptor mutants from a yeast surface-display library. *Proc Natl Acad Sci U S A*. 1999; 96:5651–6. [PubMed: 10318939]
- Kieke MC, Sundberg E, Shusta EV, Mariuzza RA, Wittrup KD, Kranz DM. High affinity T cell receptors from yeast display libraries block T cell activation by superantigens. *J Mol Biol*. 2001; 307:1305–15. [PubMed: 11292343]
- Kim HM, Park BS, Kim JI, Kim SE, Lee J, Oh SC, Enkhbayar P, Matsushima N, Lee H, Yoo OJ, Lee JO. Crystal structure of the TLR4-MD-2 complex with bound endotoxin antagonist Eritoran. *Cell*. 2007; 130:906–17. [PubMed: 17803912]
- Kobayashi M, Saitoh S, Tanimura N, Takahashi K, Kawasaki K, Nishijima M, Fujimoto Y, Fukase K, Akashi-Takamura S, Miyake K. Regulatory roles for MD-2 and TLR4 in ligand-induced receptor clustering. *Journal of immunology (Baltimore, Md : 1950)*. 2006; 176:6211–8.
- Kohara J, Tsuneyoshi N, Gauchat JF, Kimoto M, Fukudome K. Preparation and characterization of truncated human lipopolysaccharide-binding protein in *Escherichia coli*. *Protein expression and purification*. 2006; 49:276–83. [PubMed: 16839777]
- Mattis DM, Spaulding AR, Chuang-Smith ON, Sundberg EJ, Schlievert PM, Kranz DM. Engineering a soluble high-affinity receptor domain that neutralizes staphylococcal enterotoxin C in rabbit models of disease. *Protein engineering, design & selection : PEDS*. 2013; 26:133–42.
- Medzhitov R, Preston-Hurlburt P, Janeway CA Jr. A human homologue of the *Drosophila* Toll protein signals activation of adaptive immunity. *Nature*. 1997; 388:394–7. [PubMed: 9237759]
- Meng J, Drolet JR, Monks BG, Golenbock DT. MD-2 residues tyrosine 42, arginine 69, aspartic acid 122, and leucine 125 provide species specificity for lipid IVA. *The Journal of biological chemistry*. 2010a; 285:27935–43. [PubMed: 20592019]
- Meng J, Lien E, Golenbock DT. MD-2-mediated ionic interactions between lipid A and TLR4 are essential for receptor activation. *The Journal of biological chemistry*. 2010b; 285:8695–702. [PubMed: 20018893]
- Michel O, Duchateau J, Sergysels R. Effect of inhaled endotoxin on bronchial reactivity in asthmatic and normal subjects. *Journal of applied physiology (Bethesda, Md : 1985)*. 1989; 66:1059–64.
- Nagai Y, Akashi S, Nagafuku M, Ogata M, Iwakura Y, Akira S, Kitamura T, Kosugi A, Kimoto M, Miyake K. Essential role of MD-2 in LPS responsiveness and TLR4 distribution. *Nature immunology*. 2002; 3:667–72. [PubMed: 12055629]
- Oblak A, Jerala R. Species-specific activation of TLR4 by hypoacylated endotoxins governed by residues 82 and 122 of MD-2. *PloS one*. 2014; 9:e107520. [PubMed: 25203747]
- Oblak A, Jerala R. The molecular mechanism of species-specific recognition of lipopolysaccharides by the MD-2/TLR4 receptor complex. *Molecular immunology*. 2015; 63:134–42. [PubMed: 25037631]
- Ohto U, Fukase K, Miyake K, Satow Y. Crystal structures of human MD-2 and its complex with antiendotoxic lipid IVA. *Science (New York, NY)*. 2007; 316:1632–4.
- Ohto U, Fukase K, Miyake K, Shimizu T. Structural basis of species-specific endotoxin sensing by innate immune receptor TLR4/MD-2. *Proc Natl Acad Sci U S A*. 2012; 109:7421–6. [PubMed: 22532668]
- Park BS, Song DH, Kim HM, Choi BS, Lee H, Lee JO. The structural basis of lipopolysaccharide recognition by the TLR4-MD-2 complex. *Nature*. 2009; 458:1191–5. [PubMed: 19252480]
- Prajapati RS, Das M, Sreeramulu S, Sirajuddin M, Srinivasan S, Krishnamurthy V, Ranjani R, Ramakrishnan C, Varadarajan R. Thermodynamic effects of proline introduction on protein stability. *Proteins*. 2007; 66:480–91. [PubMed: 17034035]
- Prohinar P, Re F, Widstrom R, Zhang D, Teghanemt A, Weiss JP, Giannini TL. Specific high affinity interactions of monomeric endotoxin.protein complexes with Toll-like receptor 4 ectodomain. *The Journal of biological chemistry*. 2007; 282:1010–7. [PubMed: 17121827]



- Ranoa DR, Kelley SL, Tapping RI. Human lipopolysaccharide-binding protein (LBP) and CD14 independently deliver triacylated lipoproteins to Toll-like receptor 1 (TLR1) and TLR2 and enhance formation of the ternary signaling complex. *The Journal of biological chemistry*. 2013; 288:9729–41. [PubMed: 23430250]
- Re F, Strominger JL. Separate functional domains of human MD-2 mediate Toll-like receptor 4-binding and lipopolysaccharide responsiveness. *Journal of immunology (Baltimore, Md : 1950)*. 2003; 171:5272–6.
- Richman SA, Kranz DM, Stone JD. Biosensor detection systems: engineering stable, high-affinity bioreceptors by yeast surface display. *Methods Mol Biol*. 2009; 504:323–50. [PubMed: 19159105]
- Shusta EV, Kieke MC, Parke E, Kranz DM, Wittrup KD. Yeast polypeptide fusion surface display levels predict thermal stability and soluble secretion efficiency. *J Mol Biol*. 1999; 292:949–56. [PubMed: 10512694]
- Starwalt SE, Masteller EL, Bluestone JA, Kranz DM. Directed evolution of a single-chain class II MHC product by yeast display. *Protein engineering*. 2003; 16:147–56. [PubMed: 12676983]
- Teghanemt A, Re F, Prohinar P, Widstrom R, Gioannini TL, Weiss JP. Novel roles in human MD-2 of phenylalanines 121 and 126 and tyrosine 131 in activation of Toll-like receptor 4 by endotoxin. *The Journal of biological chemistry*. 2008a; 283:1257–66. [PubMed: 17977838]
- Teghanemt A, Widstrom RL, Gioannini TL, Weiss JP. Isolation of monomeric and dimeric secreted MD-2. Endotoxin.sCD14 and Toll-like receptor 4 ectodomain selectively react with the monomeric form of secreted MD-2. *The Journal of biological chemistry*. 2008b; 283:21881–9. [PubMed: 18519568]
- Trompette A, Divanovic S, Visintin A, Blanchard C, Hegde RS, Madan R, Thorne PS, Wills-Karp M, Gioannini TL, Weiss JP, Karp CL. Allergenicity resulting from functional mimicry of a Toll-like receptor complex protein. *Nature*. 2009; 457:585–8. [PubMed: 19060881]
- Tsuneyoshi N, Fukudome K, Kohara J, Tomimasu R, Gauchat JF, Nakatake H, Kimoto M. The functional and structural properties of MD-2 required for lipopolysaccharide binding are absent in MD-1. *Journal of immunology (Baltimore, Md : 1950)*. 2005; 174:340–4.
- Viriyakosol S, Tobias PS, Kitchens RL, Kirkland TN. MD-2 binds to bacterial lipopolysaccharide. *The Journal of biological chemistry*. 2001; 276:38044–51. [PubMed: 11500507]
- Visintin A, Halmen KA, Latz E, Monks BG, Golenbock DT. Pharmacological inhibition of endotoxin responses is achieved by targeting the TLR4 coreceptor, MD-2. *Journal of immunology (Baltimore, Md : 1950)*. 2005; 175:6465–72.
- Wang N, Mattis DM, Sundberg EJ, Schlievert PM, Kranz DM. A single, engineered protein therapeutic agent neutralizes exotoxins from both *Staphylococcus aureus* and *Streptococcus pyogenes*. *Clin Vaccine Immunol*. 2010; 17:1781–9. [PubMed: 20861327]
- Wills-Karp M, Nathan A, Page K, Karp CL. New insights into innate immune mechanisms underlying allergenicity. *Mucosal Immunol*. 2010; 3:104–10. [PubMed: 20032970]

### Highlights

- 1. Novel use of yeast-display for MD-2 expression enabled rapid mutational analyses
- 2. Selection of MD-2 mutants from libraries revealed importance of specific residues
- 3. Aromatic residues were strongly preferred at F119 and F121 for LPS binding
- 4. Proline mutations selected in a key loop (119–132) stabilized the protein
- 5. Charged mutations at S120 and G123 yielded enhanced ligand binding

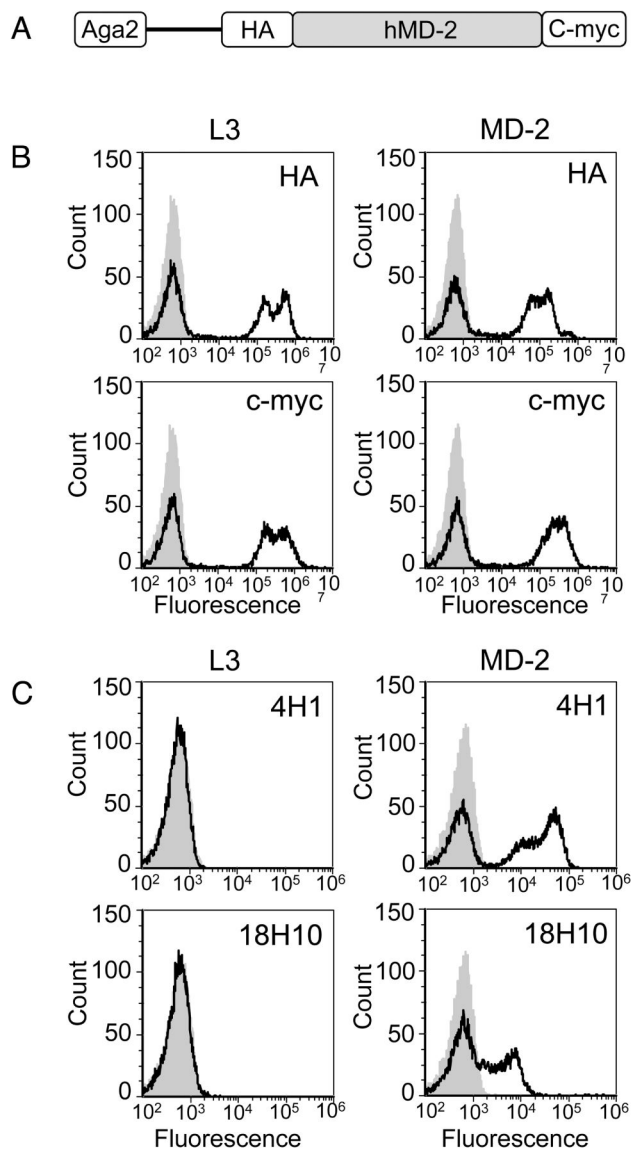


**Fig. 1. MD-2 is expressed on the surface of yeast**

(A) Structure of yeast displayed human MD-2 (hMD-2) gene. (B) Flow cytometry histograms of yeast displayed MD-2 and negative control L3, were stained with anti-HA and anti-c-myc mAbs (black outline open traces), showing yeast surface levels of N- and C-terminal expression tags. (C) Histograms of yeast displayed MD-2 and L3 staining with MD-2 specific mAbs 4H1 and 18H10 (black outline open traces). The mAbs 4H1 and 18H10 were unable to bind the negative control yeast displayed L3, but both were able to bind MD-2 as indicated by the positive fluorescence (open trace). The grey filled histogram in each graph is cells stained with secondary antibody alone and the black trace is either L3 (left column) or MD-2 (right column). Histogram profiles are representative of three or more experiments.

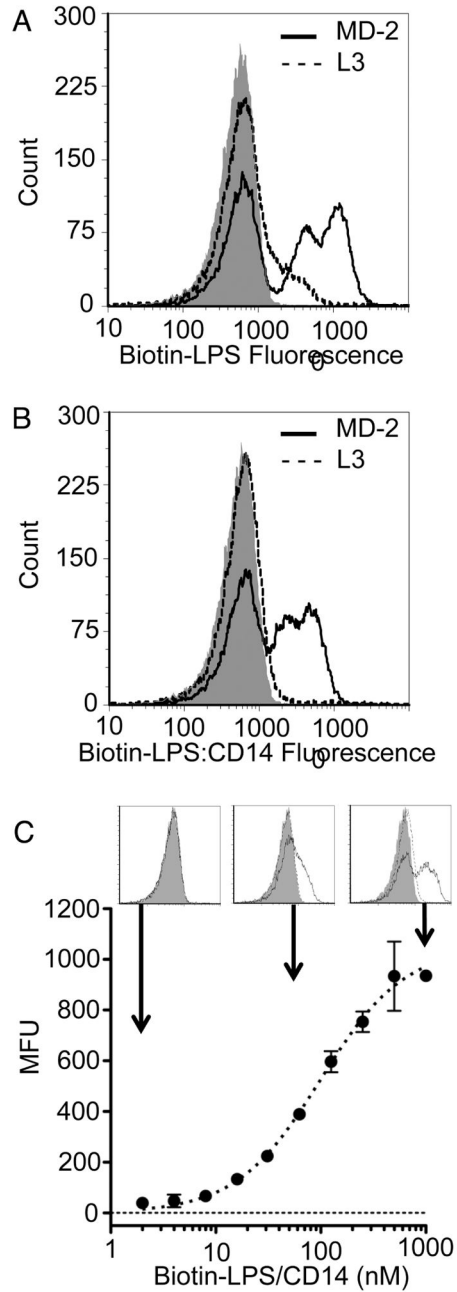


**Fig. 2. Yeast displayed MD-2 binds to biotin-LPS & CD14 reduces nonspecific biotin-LPS signal** (A) Histogram of biotin-LPS binding to yeast displayed MD-2 (solid line) and negative control L3 (dotted line) relative to secondary reagent only (grey filled histogram). (B) The nonspecific negative control signal is reduced when biotin-LPS is incubated with CD14 prior to titration with yeast displayed MD-2. (C) Biotin-LPS was incubated with CD14 after which, MD-2 was titrated with the biotin-LPS/CD14 complex. The MFU for histograms were determined at each concentration of LPS, and the background MFU was subtracted from these values. This MFU was plotted against concentration of biotin-LPS/CD14 to generate the binding curve. Insets of histograms at indicated concentrations are shown.

Histogram profiles are representative of three or more experiments. The error bars represent SEM. (n=3)

Author Manuscript

Author Manuscript

Author Manuscript

Author Manuscript

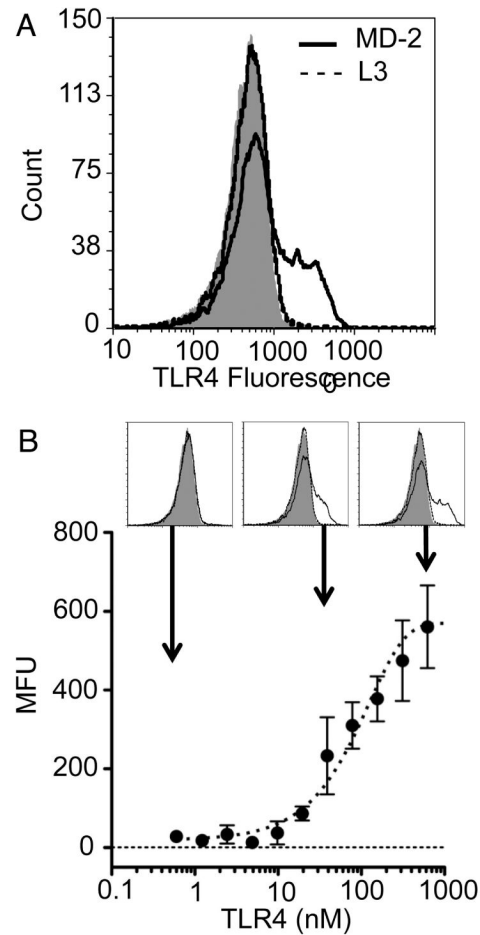


**Fig. 3. Yeast displayed MD-2 binds to TLR4**

(A) Histogram of TLR4 binding to yeast displayed MD-2 (solid line) and negative control L3 (dotted line) relative to secondary reagent only (grey filled histogram). (B) Yeast displayed MD-2 was titrated with TLR4. The MFU for histograms were determined at each concentration of TLR4, and the background MFU was subtracted from these values. This MFU was plotted against the concentration of TLR4 to generate the binding curve. Insets of histograms at indicated concentrations are shown. Histogram profiles are representative of three or more experiments. The error bars represent SEM. (n=3)



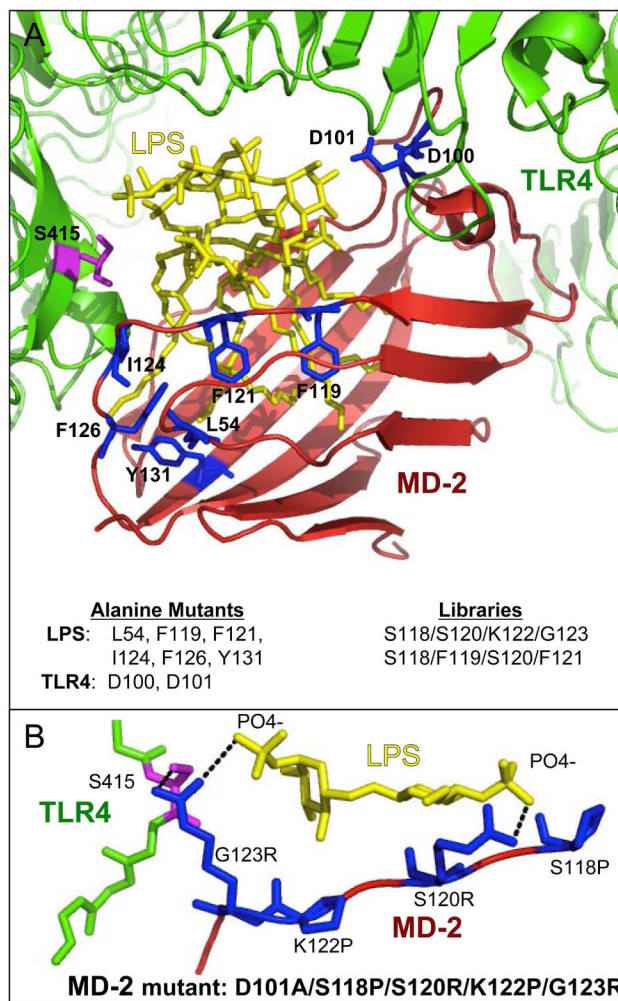


**Fig. 4. Structure and model of MD-2 binding LPS and TLR4**

(A) Structure of LPS (yellow) binding to MD-2 (red) and TLR4 (green). Selected residues are shown in blue in MD-2 and magenta in TLR4. (B) Model of MD-2 clone D101A/S118P/S120R/K122P/G123R with wild-type backbone shown in red and mutations shown in blue. Select LPS residues (yellow) and TLR4 residues (green and magenta). Mutation MD-2:G123R shows a possible charge interaction with the negative-charged LPS phosphate and a possible hydrogen bond with TLR4:S415 (magenta), that may contribute to improved stability. Mutation S120R shows a possible charge interaction with another negative-charged LPS phosphate. Library selected proline mutations S118P and K122P that also may contribute to improved stability are shown. Structure and models based on RCSB PDB accession code 3FXI.

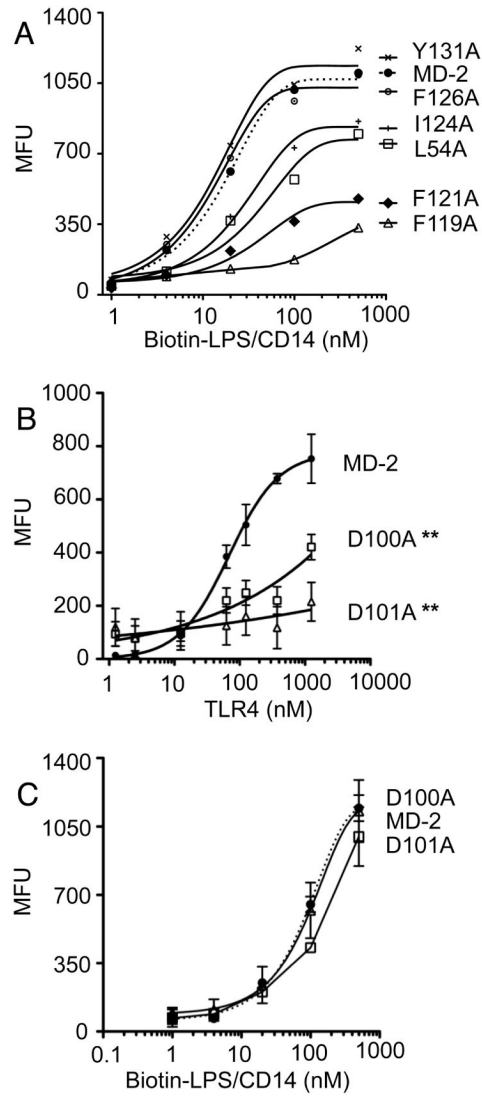


**Fig. 5. MD-2 alanine mutants**

(A) Yeast displayed MD-2 and MD-2 alanine mutants were titrated with biotin-LPS after CD14 incubation. Mutations Y131A and F126A show no change in stability or binding affinity relative to MD-2, whereas F121A and F119A show the greatest changes (results are representative of two or more independent experiments which were performed on different days using different yeast cells or different soluble protein preparations). (B) MD-2, D100A, and D101A were titrated with TLR4 and (C) biotin-LPS/CD14. Mutants D100A and D101A show statistically significant reduced binding affinity to TLR4, and retain wild-type binding affinity and stability to biotin-LPS/CD14. MFU values were determined from histograms, background values subtracted, and plotted against the appropriate ligand. The error bars represent range. (n=2 for B & C). “\*\*” Represents statistically significant binding affinity in comparison to MD-2 determined by two-tailed unpaired t-test (p<0.01).

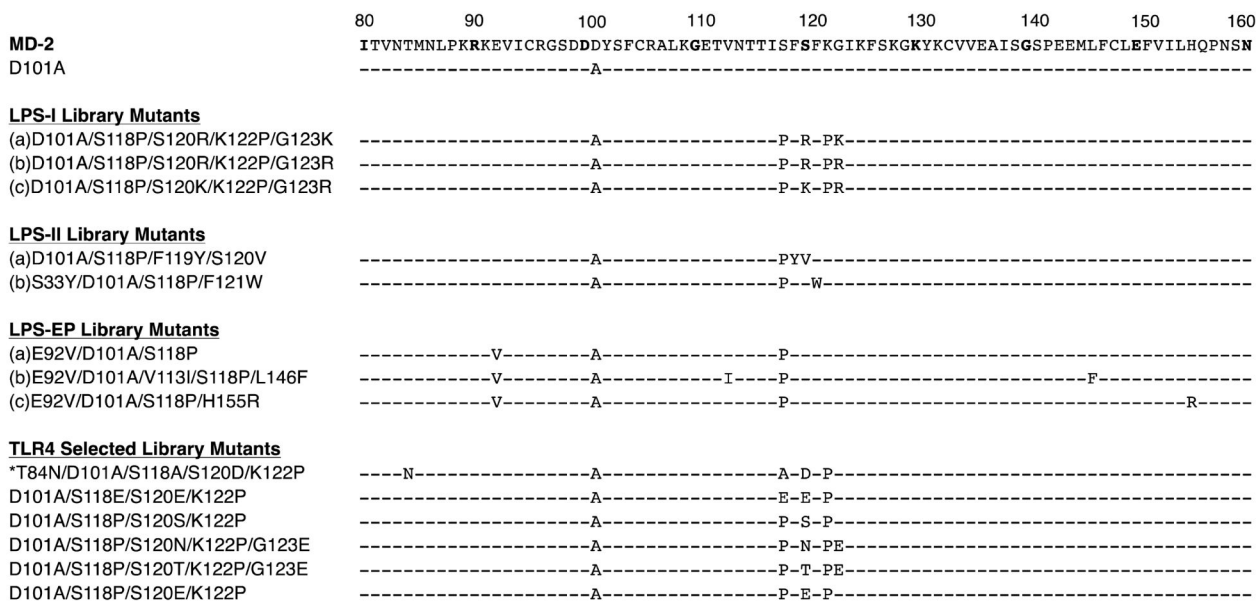


**Fig. 6. MD-2 and MD-2 mutant sequences**

MD-2 and D101A sequences, as well as sequences of mutants isolated from the fifth sorts of libraries LPS-I (S118/S120/K122/G123), LPS-II (S118/F119/S120/F121) and LPS-EP with LPS. Sequences from the fourth sort mutants and the single fifth sort mutant from the TLR4 selected library (S118/S120/K122/G123) are also shown. Sequences shown begin at residue 80. Mutation S33Y of mutant S33Y/D101A/S118P/F121W in library LPS-II not shown.

\*=Mutant identified in TLR4 selected library 4<sup>th</sup> sort and was the unique mutant sequence identified in the 5<sup>th</sup> sort.

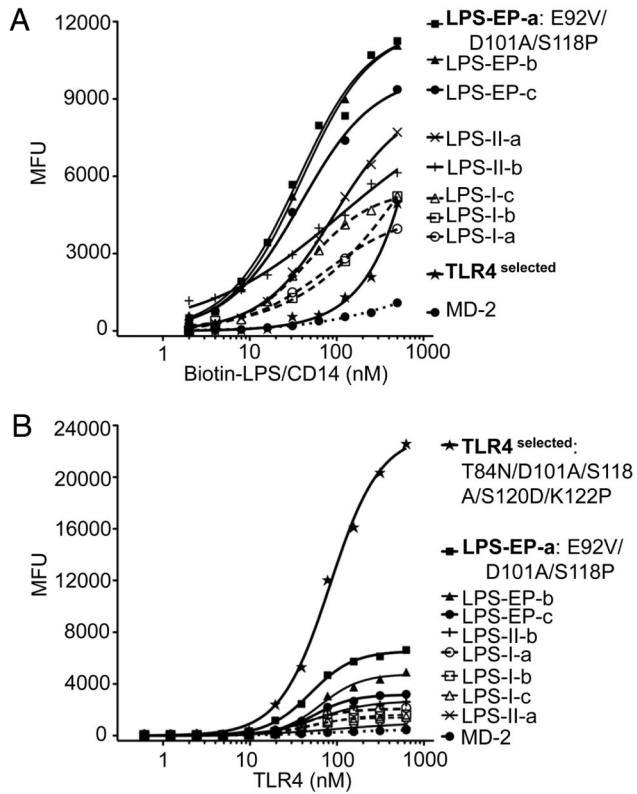


**Fig. 7. Clone analysis for biotin-LPS/CD14 and TLR4 binding**

(A) Clones were titrated with biotin-LPS/CD14, and (B) also titrated with TLR4. Stability was most improved in LPS-EP mutants, followed by LPS-II, and least for LPS-I mutants in biotin-LPS/CD14 studies in comparison to MD-2, with a similar trend for TLR4 studies with the exception of the TLR4 selected mutant showing the greatest improvement. Mutant LPS-EP-a (E92V/D101A/S118P) had the most improved stability in biotin-LPS/CD14 studies, while mutant TLR4 selected (T84N/D101A/S118A/S120D/K122P) showed the greatest improvements in stability in TLR4 studies. There were no significant differences in binding affinity from MD-2, except for TLR4 selected binding to biotin-LPS/CD14. (Results shown are representative of three experiments repeated at different concentrations).

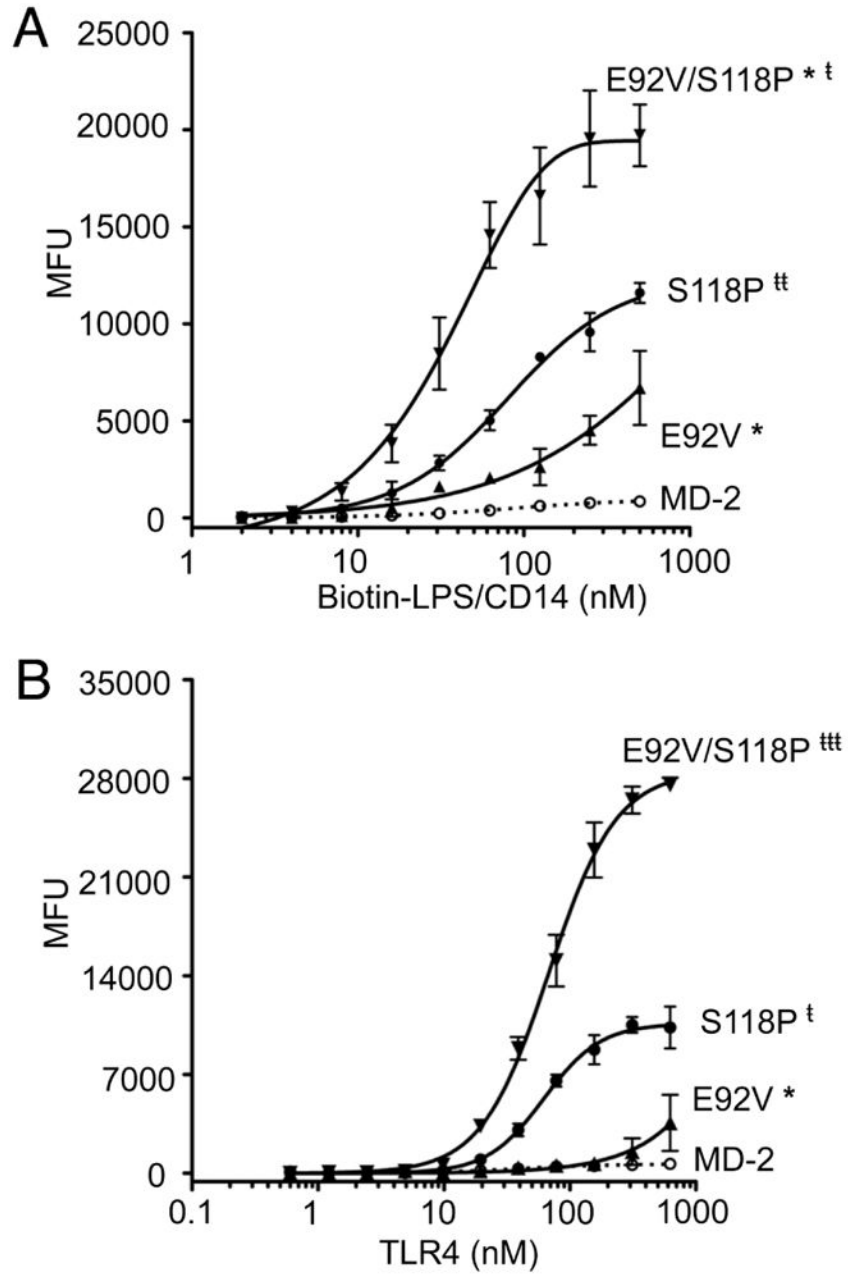


**Fig. 8. Select clone analysis for biotin-LPS/CD14 and TLR4 binding**

(A) Clones E92V, S118P, and E92V/S118P were titrated with biotin-LPS/CD14, and (B) also titrated with TLR4. The maximum MFU as determined with biotin-LPS/CD14 and TLR4 for the double mutant E92V/S118P was improved compared to either mutation individually. Error bars represent range (n=2 per group). “\*” Represents statistically significant binding affinity in comparison to MD-2 determined by two-tailed unpaired t-test (p<0.05). “†” represents statistically significant maximum MFU saturation in comparison to MD-2 determined by two-tailed unpaired t-test (†: p<0.05, ††: p<0.01, †††: p<0.001), E92V in 8A and 8B do not reach saturation.